Impact of Oxetane Incorporation on the Structure and Stability of Alpha-helical Peptides

Eleanor S. Jayawant[a], Jonathan D. Beadle[a], Ina Wilkening[a], Piotr Raubo[b], Michael Shipman[a],

Rebecca Notman[a] and Ann M. Dixon[a*]

Running Title: Oxetane incorporation into the backbone of α-helix

[a] Department of Chemistry, University of Warwick, Coventry, CV4 7AL, UK.

[b] Medicinal Chemistry, Research and Early Development, Oncology R&D, AstraZeneca, Cambridge, UK.

*To whom correspondence should be addressed: Dr Ann Dixon, Department of Chemistry, University of Warwick, Coventry, CV4 7AL, UK, Telephone: +44 2476 150037; FAX: +44 2476 524112; email: ann.dixon@warwick.ac.uk,

ABSTRACT

Peptide-based drugs combine advantages of larger biological therapeutics with those of small molecule drugs, but they generally display poor permeability and metabolic stability. Recently, we introduced a new type of peptide bond isostere, in which the backbone carbonyl is replaced with a 3-amino oxetane heterocycle, into short linear peptides with the aim of improving their therapeutic potential. In this study, we have explored the impact of oxetane modification on α-helical peptides to establish whether or not this modification is tolerated in this biologically important structural motif. The oxetane modification was introduced at two positions in a well-characterised helical peptide sequence, and circular dichroism and NMR spectroscopy were used to measure the resulting secondary structure content under different experimental conditions. Our data demonstrated that introduction of an oxetane into the peptide backbone results in a significant loss of helicity, regardless of where in the sequence the modification is placed. The molecular determinants of this destabilisation were then explored using steered molecular dynamics simulations, a computational method analogous to single molecule spectroscopy. Our simulations indicated that oxetane modification introduces a kink in the helical axis, alters the dihedral angles of residues up to three positions away from the modification, and disrupts the (i, i+4) hydrogen bonding pattern characteristic of α-helices in favour of new, short-range hydrogen bonds. The detailed structural understanding provided in this work can direct future design of chemically modified peptides.

KEYWORDS

INTRODUCTION

Chemical modification of peptides for improved bioavailability and metabolic stability is a critical aspect of work in the development of peptide-based drugs.[1] Introduction of non-natural backbone linkages such as thioamides, azapeptides (where the Cα is replaced with a nitrogen) and poly-N-substituted glycines (peptoids), amongst others, has led to the increased stability or enhanced bioavailability of a wide range of peptides.[2–6] However, backbone modification has also been shown to fundamentally change the structural properties of polypeptide chains, and no one modification has been shown to be universally tolerated. For this reason, an improved understanding of the impact of available modifications is of critical importance to future development of peptide-based medicines.

Oxetanes are well-established bioisosteres in medicinal chemistry.[7] Grafting the oxetane motif onto small molecules in place of carbonyl or gem-dimethyl groups can trigger profound changes in metabolic stability, lipophilicity, aqueous solubility and conformational preference without drastically changing hydrogen bonding capabilities or lone pair arrangement,[8,9] despite the fact that the C…O distance in the oxetane ring is longer than in a carbonyl group (2.1 Å vs. 1.2 Å)[7]. Oxetanes have emerging applications in peptide science.[10] For example, grafting of oxetanes onto cysteine side chains has been shown to significantly improve the stability and activity of proteins and antibodies.[11,12]

Oxetanes have been grafted into the peptide backbone, where the backbone amide C=O of an amino acid is substituted with a four-membered oxetane ring.[10,13–15] Oxetane incorporation into short peptides has previously been shown by us to lead to improvements in head-to-tail cyclisations in a range of tetra-, penta-, hexa- and

heptapeptides, in a superior manner to other common backbone modifications. This appears to be due to the formation of a turn in proximity to the modification, as evidenced by the presence of long-range NOEs.[16] However, it remains unknown as to how well-tolerated oxetane modifications are in other, more regular, structural motifs such as β-sheets and α-helices.

The α-helix is a ubiquitous secondary structure motif in peptides and proteins, and plays a multitude of biological roles including structural scaffold,[17] cell signalling initiator,[18] and membrane curvature sensor[19] amongst others. Furthermore, the ability of α-helices to disrupt protein-protein interactions and to destroy the integrity of cell membranes makes them desirable drug candidates.[20,21] α-Helical structures have a characteristic repeating hydrogen bond pattern, where each carbonyl oxygen forms a hydrogen bond with a backbone amide hydrogen four residues away. Although replacement of a carbonyl with an oxetane is a relatively conservative modification, as the two groups have similar hydrogen bonding capabilities, the difference in size and change in dihedral angles may substantially affect the $i, i+4$ hydrogen bonding pattern integral for helix stability. It is therefore of considerable interest to explore the impact of oxetane modification on the viability and stability of this biologically relevant structural element.

In this work we investigate the effects of replacing one of the alanine residues in a well-characterised α-helical peptide sequence[22] with an oxetane-modified alanine (A_{ox}) or glycine (G_{ox}). Using nuclear magnetic resonance and circular dichroism (CD) spectroscopy, we explored the impact of incorporation of an oxetane-modified alanine at two different sites, and an oxetane-modified glycine at a single site, in an α-helical structure. These two sites represented a central modification (residue 8) and a

4

modification towards the N-terminus of the peptide (residue 3), and were selected based on previous research involving modifications of α-helical structures, which suggest that modifications are better tolerated in the terminal regions of α-helices due to their lower intrinsic helical content.[22,23] We observe that the oxetane modification is very poorly tolerated in an α-helix, regardless of where it is placed, and destabilizes helical regions up to four residues away depending on the solvent used. This destabilisation is not improved when the residue type is changed to a more conformationally flexible Gly. Using steered molecular dynamics (SMD) computer simulations, we reveal the molecular details of this effect in order to guide future design of chemically modified peptides.

EXPERIMENTAL METHODS

Circular Dichroism

CD experiments were performed on a Jasco model J-815 spectropolarimeter with temperature control. Samples for CD were prepared by dissolving peptides[15] to a final concentration between 34-192 µM in either 10 mM potassium phosphate buffer with 1 M NaCl, pH 7.0, 80% MeOH, or 100% MeOH. Spectra were recorded in a 0.1 cm path length cuvette between 250 and 180 nm using a 1.0 nm pitch, 1.0 nm band width, a 1 s response time, and a scanning speed of 100 nm/min. Spectra were acquired at temperatures of either 5°C (10 mM KPi buffer and 80% MeOH) or 0°C (100% MeOH), allowing 10 min equilibration time before CD spectra were recorded. Each spectrum represents the average of 10 scans. All CD data were converted to units of mean residue

ellipticity, and secondary structure content was estimated by fitting of the data using the DichroWeb software[24] (Selcon3, reference sets 3 and 4).

NMR Experiments

All NMR experiments were performed in 3 mm NMR tubes (Bruker, Germany) on an Avance 700 MHz spectrometer (Bruker Biospin, UK) equipped with a triple resonance inverse cryoprobe with Z-gradients. Data were processed using Topspin 4.0.7 (Bruker Biospin), and analysed using Sparky[25]. Peptides were prepared by dissolving the peptide to a final concentration of 2 mM in 80% MeOD-d_4 + 20% H_2O. ^1H-^1H TOCSY and NOESY NMR spectra were recorded with 4096 × 256 data points (zero-filled to 8192 x 512 in procpars), 32 scans, a spectral width of 14 ppm in both dimensions at a temperature of 10°C. TOCSY and NOESY mixing times ranged from 70-140 ms and 100-200 ms, respectively.

Molecular dynamics simulations

Steered molecular dynamics (SMD) simulations were carried out on the four helical peptides in methanol. Starting coordinates of the peptides were generated using Avogadro,[26] built assuming an ideal α-helical conformation with N-terminal acetyl and C-terminal amide caps. All simulations were performed using the Gromacs 5.1.4 simulation package[27] using the CHARMM27 force field[28] with modifications for the oxetane ring[13] for the peptides and the CHARMM general force field for methanol.[29] Each peptide was simulated ten times for 40 ns at 300 K with different initial co-ordinates. The peptides were anchored at the N-terminal Cα with a dummy spring pulling the C-terminal Cα. The dummy spring was pulled with a constant velocity

of 0.00025 nm ps^{-1} and a force of 25 kJ mol^{-1} nm^{-2}. Initial tests to determine the optimum choice of pulling velocity and spring constant are included in the Supplementary Information. Under these conditions, each peptide unwinds within ca. 20 ns. Full details of simulation parameters are provided in Supplementary Information.

RESULTS AND DISCUSSION

Oxetane substitution leads to long-range destabilization of α-helices

To investigate the impact of a single oxetane modification at various positions within an α-helical region, we selected a well-characterised alanine-based model peptide, the sequence of which is given in Table 1 (**1**). This peptide is known to be monomeric,[30] ~70% α-helical,[23,31] and has been shown to unfold in the presence of other peptide backbone substitutions such as a thioamide substitution.[22] Site specific modifications were made to this Ala-rich model peptide through introduction of an oxetane-modified Ala residue (A$_{ox}$) in the centre of the helical region at position 8 (Table 1 **2a**), or near the N-terminus at position 3 (Table 1 **2b**); or an oxetane-modified Gly residue (G$_{ox}$) at position 3 (Table 1 **2c**). Substitution at these positions allowed direct comparison to the data reported by Reiner and coworkers[22] for this same sequence, in which the identical positions were modified with thioamide. The solid-phase synthesis of these peptides has been described elsewhere.[15]

The impact of oxetane modification on peptide fold was studied using circular dichroism (CD) spectroscopy in two different solvents (Figure 1). Initially, CD spectra were collected for peptides solubilised in potassium phosphate buffer (pH 7.0) at 5°C in

order to directly compare the impact of oxetane modification to that observed for the thioamide-modified peptide (for which all CD data were collected at 5°C).[22] Secondary structure content was estimated by fitting of the data using the DichroWeb software,[24] and the resulting values are given in Table 1. The helical content of the alanine-based model peptide in potassium phosphate buffer (58%) was slightly lower than that reported previously in the same buffer (68%),[30] however this may reflect the uncertainties inherent in fitting of peptide data using reference sets predominantly composed of larger proteins. Regardless, the 10% difference we report here accounts for only 1–2 amino acid residues. Incorporation of an oxetane-modified alanine either at the centre or at the N-terminus of the model peptide (**2a** and **2b,** respectively) lead to a pronounced reduction in helical content (Figure 1A) to between 4–9% helicity. Incorporation of a G_{ox} at the N-terminus of the peptide (**2c**) resulted in a similar decrease in helicity. This estimate of helical content allowed us to compare the relative loss of helicity in terms of numbers of residues unfolded by each substitution, as summarized in Table 1. The CD data indicated that the parent peptide **1** contained approximately ten helical residues before modification, and the oxetane modification lead to unfolding of 8–9 helical residues, clearly demonstrating that the oxetane substitution has a highly destabilising and unexpectedly long-range effect when placed within an α-helix.

The data obtained in phosphate buffer yielded similar levels of helical unfolding regardless of where the oxetane was placed in the sequence. To explore the solvent-sensitivity and the position-dependence of this effect, we sought a solvent that would stabilise the helical fold adequately to reveal any further differences. Given that methanol is known to induce helicity in peptides and proteins,[32] the oxetane-modified peptides were

expected to show an increase in helical content in this solvent compared to the previous observations in buffer. Therefore, CD spectra were acquired for the parent and modified peptides in 80% MeOH at 5°C, and the resulting data are shown in Figure 1B and Table 1. While the helical content of the parent peptide **1** was very similar in 80% MeOH (56%), incorporation of the oxetane modification did not lead to complete unfolding in this solvent, but instead lead to partial unfolding that was dependent on the location of the modification (Figure 1B). Unfolding was less pronounced when the substitution was made near the N-terminus of the peptide (**2b** and **2c**), with approximately 4–5 residues unfolded upon introduction of the oxetane. Incorporation of an oxetane at the centre of the helix (**2a**) "unfolds" approximately double the number of residues (8 residues). This same trend was observed for peptides dissolved in 100% MeOH at 0°C (the temperature that yielded maximal helical content in this solvent) as shown in Table 1 and Figure 1C, revealing more clearly the position-dependence and range of the oxetane-mediated unfolding.

Peptides **1** and **2c** were also analysed using solution state nuclear magnetic resonance spectroscopy. ^{1}H-^{1}H TOCSY and NOESY data were acquired for samples in 80% MeOD-d_4, and assignment was attempted. The repetitive nature of the sequence precluded full sequential assignment, however all four Lys residues in the peptide were well-resolved and the unique Gly and Tyr residues were readily assigned, as was the oxetane-modified Gly in **2c**. NOEs were used where possible to sequentially assign additional residues, but signals from the majority of the Ala residues were heavily overlapped and identification of unique i, i+4 NOE correlations (characteristic of α-helix formation) was not possible. NMR spectra for **1** and **2c** are given in Figures S1-S4, and

resulting assignments for both peptides are shown in Table 2. The Hα chemical shifts were then used as chemical probes for changes in chemical environment at regular points along the length of the peptide chain. As described by the chemical shift index (CSI) method,[33,34] it is well-known that the Hα chemical shift is very sensitive to changes in secondary structure. The Hα chemical shifts of residues 15-18, distant from the oxetane modification, remained unchanged to within 0.01 ppm upon introduction of the oxetane. In contrast, a significant downfield shift of ≥ 0.21 ppm for the Lys 1 Hα peak was observed (from 4.02 - 4.05 ppm in **1** to 4.26 ppm in **2c**) upon introduction of the oxetane modification at position 3. A similar downfield shift of ≥ 0.17 ppm was also observed for one additional Lys residue (either Lys 6 or Lys 11) from 4.02 - 4.05 ppm in **1** to 4.22 ppm in **2c**. According to the CSI method, a downfield shift for an Hα proton signal of 0.1 ppm or more suggests a change in secondary structure from an α-helix to an unstructured (random coil) chain, reflecting the differences in ^{1}H chemical environment and hydrogen bonding patterns in regions of helical structure. This relationship, alongside our results from CD above, suggests that Lys 1, 6 and/or 11 are all in an α-helical environment in peptide **1**, whereas only one Lys (either Lys 6 or 11) is in an α-helical environment in peptide **2c**.

Work required to unwind oxetane-modified helices reflects a weakening of the fold

The stability of a protein fold is reflected in the energy that is required to unfold the protein. To assess the change in stability of the helical fold in the absence and presence of an oxetane modification, we have utilised a method called steered molecular dynamics (SMD). In SMD, a molecule is anchored at a fixed point, and pulled at another point via a dummy spring, in a manner analogous to single molecule spectroscopy. It has

previously been used to aid unwinding of helical structures,[35,36] as it allows unwinding events to occur on computationally feasible timescales. Integration of the resulting force-extension curves produced during the SMD simulations over a 20 ns period yields the work required to unwind each helix, which directly reflects the stability of the helical fold.

We built models of peptides **1–2** restrained to an idealised α-helical conformation (φ of -60°, ψ of -40°), solvated in a pre-equilibrated box of methanol and counter-ions, and equilibrated in two stages using the *NVT* (constant number of particles, volume and temperature) and *NPT* (constant number of particles, pressure and temperature) ensembles. Unwinding was then initiated by releasing the position restraints, anchoring the N-terminus and pulling a dummy spring from the C-terminus at a speed of 0.00025 nm ps^{-1} and a force of 25 kJ mol^{-1} nm^{-2} over 40 ns. These parameters were selected following a series of tests in which spring constants of 100 to 10 kJ mol^{-1} nm^{-2} and pull speeds of 0.02 to 0.00005 nm ps^{-1} were assessed (Figure S5). Further details of parameter optimisation are described in the Supplementary Information. Ten repeats were sufficient for the data to converge (see Figure S6). Figure 2 shows the amount of work required to unwind each helix five nm as derived from integration of force extension curves averaged over the ten repeats. The work required to unwind the helix in the parent peptide **1** was estimated at 127.2 kJ mol^{-1}. Introduction of A_{ox} near the N-terminus (at position 3, peptide **2b**) decreased the amount of work required to unwind the helix five nm by 15.9 kJ mol^{-1} (total work = 111.3 kJ mol^{-1}). Similarly, introduction of G_{ox} at position 3 (peptide **2c**) decreased the amount of work required compared to the parent peptide **1** by 10.4 kJ mol^{-1} (total work = 116.8 kJ mol^{-1}). The difference between the work required to unwind

peptides **2b** and **2c** five nm is statistically significant (p < 0.02, independent samples t-test), suggesting that the fold of peptide **2c** is moderately more stable. Oxetane incorporation at the central residue (position 8, peptide **2a**) had the greatest impact, and further decreased the work required to unwind the helix by ~ 30 kJ mol^{-1} (total work = 97.3 kJ mol^{-1}).

The SMD data agrees with the trend observed in the CD data, and indicates that the introduction of an oxetane into a highly helical region destabilizes the fold by up to 30 kJ mol^{-1}. For reference, the difference in energy between the native and unfolded state of a protein is typically in the region of 20–40 kJ mol^{-1}.[37] Therefore, oxetane is highly destabilising when inserted into a helical region, resulting in destabilisation several times higher than that caused by amino acid mutation,[38] or corresponding to the loss of multiple strong hydrogen bonds.[39] In comparison, thioamide introduction in the same position resulted in destabilisation of the fold by ~7 kJ mol^{-1},[22] due to the longer C=S bond (1.56 Å)[40] and larger sulphur atom.

The trend observed when comparing **2b** and **2c** is slightly unexpected, as glycine is considered disruptive in internal helical positions due to its high conformational flexibility, compared to alanine which is considered stabilising.[41] It may be the case that glycine's flexibility and lack of bulky sidechain allow it to slightly compensate for the oxetane behaving as a conformational lock. However any compensation effect is minor, as ultimately the differences in helicity between **2b** and **2c** as measured by CD, and the differences in work required to unwind the two peptides as calculated using SMD, are small.

Structural implications of oxetane modification in α-helices

The SMD results above demonstrate a large destabilisation of the helical fold by introduction of a single oxetane modification. To explore the molecular determinants for this instability, we examined the atomistic models of all three peptides over the course of the simulation. During the first 5 ns of the SMD simulations, the helices relaxed away from the ideal helical structure to which they were initially restrained, although peptide **1** remained highly helical. Visual inspection of the trajectory during this initial stage of the simulation shows that oxetane modification has a clear impact on the structure and hydrogen-bonding pattern of the helical peptides. Figure 3 shows representative snapshots of peptide structures taken after 5 ns of simulation time. This time point was selected as the position restraints were removed, allowing the peptides to relax, but initial numbers of hydrogen bonds were maintained (suggesting pulling is not yet affecting the structure of the peptides). As seen in the structures, there is distortion of the helical axis near the oxetane modification in peptides **2a**–**2c**, which appears to produce a kink in the helix thus changing the hydrogen-bonding pattern. This kinking effect may reflect the oxetane acting as a β-turn-inducing element, as we recently observed in short linear oxetane-modified peptides.[16] In **1**, hydrogen bonds between the ith residue and residue $i+4$ characteristic of an α-helix are maintained, while in the oxetane-modified peptides these hydrogen bonds are quickly lost. Instead, additional i, $i+2$ hydrogen bonds are formed in proximity to the modification.

One of the characteristic properties of an α-helix is that all the amino acids have negative φ and ψ torsion angles, typically around -60° and -40° respectively. Ramachandran plots were prepared for the time period corresponding to 2–5 ns of the

trajectory. These time points were selected using the rationale that, during the first 2 ns of the simulation, peptides were relaxing from their position-restrained ideal α-helix starting configurations, while after 5 ns the structures would be strongly affected by the pulling. Figure 4A compares the Ramachandran plots of peptides **1**, **2b** and **2c**, and Figure 4B compares the Ramachandran plots of peptides **1** and **2a**. While residues 3 to 11 of the parent peptide **1** correspond to the characteristic φ and ψ angles expected for an α-helix, in the presence of the oxetane modification there is a clear distortion in dihedral angles that extends for two to three residues in either direction from the site of modification.

We compared the sampling of φ/ψ space in a G_{ox} residue between peptide **2c** and a short linear pentapeptide $LAG_{ox}AY$-OMe previously characterised by us.[16] Although it is difficult to directly compare the dihedral angles observed in peptides **2b-c** to those in $LAG_{ox}AY$-OMe due to differences in solvent, methodology and starting structures, there are some similarities in the Ramachandran plots (Figures 4 and S7). Introduction of an oxetane modification in all cases results in a splitting of the φ/ψ space sampled, with two populations appearing: one with a negative φ/negative ψ, and the second with a φ of -120 to -180° and a positive ψ angle. Interestingly, the sampling of the φ/ψ space in the G_{ox} residue of $LAG_{ox}AY$-OMe appears more similar to that of the A_{ox} in **2b** than to the G_{ox} in **2c**, however these differences may be arising due to fundamental differences in the systems as previously described.

For the four helical peptides, the number of hydrogen bonds per residue was also calculated and plotted as a function of time for the entire 20 ns SMD simulation. Representative plots are shown in Figure 5 (plots for repeat simulations are shown in Figure S8). In the parent peptide **1**, most residues form on average 1 hydrogen bond per

residue. At the start of the simulation, there is evidence of unwinding of the helix at the N-terminus, and as pulling proceeds the peptide predominantly unwinds from its C-terminus.

Oxetane modification at position 3 (**2b** and **2c**) causes a disruption in the formation hydrogen bonds four residues away (i.e. up to residue 7) as shown in Figure 5. In the case of peptide **2c**, the hydrogen bonds appear to be maintained for longer compared to **2b**, although there is a clear disruption in *i, i*+4 hydrogen bonds downstream of the modification. For peptide **2b**, the disruption of the hydrogen bonding network is also visible in the snapshots taken at 5 ns (Figure 3) and later in the trajectory, as shown in Figure 6B, where the N-terminus of the peptide adopts a largely extended conformation. As pulling proceeds, unwinding again occurs from the C-terminus. In the centrally modified peptide **2a** (modification at residue 8), the hydrogen bonding patterns in the middle of the peptide are disrupted (Figure 5), and there is a kinking effect in the helix, particularly obvious after 10 ns (Figure 6C). Like **1**, **2a** tends to unwind slightly at the N-terminus, and then predominantly from the C-terminus, although it appears that oxetane modification promotes unwinding of the central region of the peptide, as this region unwinds more readily in **2a** than in **1**.

The disruption in hydrogen bonding described by both the number of hydrogen-bonds per residue and the key unwinding events are consistent with the experimental data and suggest that the oxetane modification destabilizes α-helicity by preventing the formation of the *i*, *i*+4 hydrogen bonds characteristic of an α-helix, as evidenced by their noticeable absence in proximity to the modification in the SMD structures.

CONCLUSIONS

In this work we sought to establish whether the oxetane modification was tolerated in an α-helix, one of the most important and therapeutically relevant structural motifs in biology. Using circular dichroism and NMR spectroscopy, we have shown experimentally that the oxetane modification is highly disruptive to the helical fold and poorly tolerated in an α-helical structure. We were able to replicate the observed experimental trend using steered molecular dynamics to calculate the amount of work required to unwind each peptide, and analysis of the simulations suggests that the disruption to helicity is caused by changes in dihedral angles and hydrogen bonding patterns in proximity to the modification, due to the identity and size of the hydrogen bonding groups involved. While the α-helical structure is well-adapted to amide and carbonyl groups, backbone modification of an α-helix is not necessarily always disruptive—in fact, some backbone modifications have been shown to increase or induce helicity. For example, introduction of lactam bridges between i, i+4 amino acids has been shown to improve helix stability and bioactivity of human parathyroid hormone.[42] A more drastic backbone substitution, the replacing of a dipeptide in an α-helix with a leucine-derived 1,2,3-triazole ε^2-amino acid, results in the modified peptides retaining much of the helical structure of the parent sequence.[43] Therefore, it would appear that as long as a modification is able to maintain i, i+4 hydrogen bonds, helix disruption is minimal, suggesting that helix modifications should be considered from a hydrogen bonding perspective, rather than how structurally conservative they may first appear.

Our data suggest that oxetane substitution disrupts helicity by changing the dihedral angles of the peptide backbone in the vicinity of the modified residue, such that

they tend towards a β-turn and therefore disrupt the *i*, *i*+4 hydrogen bonds known to be vital for helix stability. This is consistent with our previous work, which suggests that in short linear peptides, the oxetane modification acts as a β-turn-inducer.[13,16] Other factors associated with the modified residue such as its increased molecular volume and different orientation of the oxygen lone pairs likely contribute to these distortions seen in the peptide backbone.

The work presented here demonstrates, for the first time, that oxetanes are not a useful modification for helical structures. To date, this modification remains best-tolerated in peptides containing secondary structure involving turns, such as α-hairpins or β-turns, where we have demonstrated that the oxetane can enhance cyclisation efficiency and stabilise turn elements in peptides.[13,16] A particularly promising direction is the use of oxetane modification to stabilise or mimic β-turn structures. β-turn structural motifs are widespread in proteins, have been implicated in molecular recognition and protein-protein interactions for proteins including GPCRs[44] and amyloid-β,[45] and are of considerable interest in the field of peptidomimetics for therapeutic use.

CONFLICTS OF INTEREST

There are no conflicts to declare.

ACKNOWLEDGEMENTS

computing facilities were provided by the University of Warwick Scientific Computing

Research Technology Platform.

REFERENCES

1   A. F. B. Räder, M. Weinmüller, F. Reichart, A. Schumacher-Klinger, S. Merzbach, C. Gilon, A. Hoffman and H. Kessler, Orally Active Peptides: Is There a Magic Bullet?, *Angew. Chemie - Int. Ed.*, 2018, **57**, 14414–14438.

2   L. Gentilucci, R. De Marco and L. Cerisoli, Chemical Modifications Designed to Improve Peptide Stability: Incorporation of Non-Natural Amino Acids, Pseudo-Peptide Bonds, and Cyclization, *Curr. Pharm. Des.*, 2010, **16**, 3185–3203.

3   A. Zega, Azapeptides as Pharmacological Agents, *Curr. Med. Chem.*, 2005, **12**, 589–597.

4   R. N. Zuckermann and T. Kodadek, Peptoids as potential therapeutics, *Curr. Opin. Mol. Ther.*, 2009, **11**, 299–307.

5   G. M. Pauletti, S. Gangwar, T. J. Siahaan, J. Aubé and R. T. Borchardt, Improvement of oral peptide bioavailability: Peptidomimetics and prodrug strategies, *Adv. Drug Deliv. Rev.*, 1997, **27**, 235–256.

6   A. A. Vinogradov, Y. Yin and H. Suga, Macrocyclic Peptides as Drug Candidates: Recent Progress and Remaining Challenges, *J. Am. Chem. Soc.*, 2019, **141**, 4167–4181.

7   J. A. Bull, R. A. Croft, O. A. Davis, R. Doran and K. F. Morgan, Oxetanes: Recent Advances in Synthesis, Reactivity, and Medicinal Chemistry, *Chem. Rev.*, 2016, **116**, 12150–12233.

8   G. Wuitschik, M. Rogers-Evans, K. Müller, H. Fischer, B. Wagner, F. Schuler, L. Polonchuk and E. M. Carreira, Oxetanes as Promising Modules in Drug Discovery, *Angew. Chemie*, 2006, **45**, 7900–7903.

9   G. Wuitschik, E. M. Carreira, B. Wagner, H. Fischer, I. Parrilla, F. Schuler, M. Rogers-Evans and K. Müller, Oxetanes in drug discovery: Structural and synthetic insights, *J. Med. Chem.*, 2010, **53**, 3227–3246.

10   G. P. Möller, S. Müller, B. T. Wolfstädter, S. Wolfrum, D. Schepmann, B. Wünsch and E. M. Carreira, Oxetanyl Amino Acids for Peptidomimetics, *Org. Lett.*, 2017, **19**, 2510–2513.

11   O. Boutureira, N. Martínez-Sáez, K. M. Brindle, A. A. Neves, F. Corzana and G. J. L. Bernardes, Site-Selective Modification of Proteins with Oxetanes, *Chem. - A Eur. J.*, 2017, **23**, 6483–6489.

12   N. Martínez-Sáez, S. Sun, D. Oldrini, P. Sormanni, O. Boutureira, F. Carboni, I. Compañón, M. J. Deery, M. Vendruscolo, F. Corzana, R. Adamo and G. J. L. Bernardes, Oxetane Grafts Installed Site-Selectively on Native Disulfides to Enhance Protein Stability and Activity In Vivo, *Angew. Chemie - Int. Ed.*, 2017, **56**, 14963–14967.

13   N. H. Powell, G. J. Clarkson, R. Notman, P. Raubo, N. G. Martin and M. Shipman, Synthesis and structure of oxetane containing tripeptide motifs, *Chem. Commun.*, 2014, **50**, 8797.

14   J. D. Beadle, A. Knuhtsen, A. Hoose, P. Raubo, A. G. Jamieson and M. Shipman, Solid-

Phase Synthesis of Oxetane Modified Peptides, *Org. Lett.*, 2017, **19**, 3303–3306.

15 S. Roesner, J. D. Beadle, L. K. B. Tam, I. Wilkening, G. J. Clarkson, P. Raubo and M. Shipman, Development of oxetane modified building blocks for peptide synthesis, *Org. Biomol. Chem.*, 2020, **18**, 5400–5405.

16 S. Roesner, G. J. Saunders, I. Wilkening, E. Jayawant, J. V. Geden, P. Kerby, A. M. Dixon, R. Notman and M. Shipman, Macrocyclisation of small peptides enabled by oxetane incorporation, *Chem. Sci.*, 2019, **10**, 2465–2472.

17 A. P. Kornev, S. S. Taylor and L. F. Ten Eyck, A helix scaffold for the assembly of active protein kinases, *Proc. Natl. Acad. Sci. U. S. A.*, 2008, **105**, 14377–14382.

18 M. A. Lemmon and J. Schlessinger, Cell signaling by receptor tyrosine kinases, *Cell*, 2010, **141**, 1117–1134.

19 R. L. Brooks and A. M. Dixon, Revealing the mechanism of protein-lipid interactions for a putative membrane curvature sensor in plant endoplasmic reticulum, *Biochim. Biophys. Acta - Biomembr.*, 2020, **1862**, p.183160.

20 I. Saraogi and A. D. Hamilton, α-Helix mimetics as inhibitors of protein-protein interactions, *Biochem. Soc. Trans.*, 2008, **36**, 1414–1417.

21 S. R. Dennison, J. Wallace, F. Harris and D. A. Phoenix, Amphiphilic α-Helical Antimicrobial Peptides and Their Structure/Function Relationships, *Protein Pept. Lett.*, 2005, **12**, 31–39.

22 A. Reiner, D. Wildemann, G. Fischer and T. Kiefhaber, Effect of thioxopeptide bonds on α-helix structure and stability, *J. Am. Chem. Soc.*, 2008, **130**, 8079–8084.

23 A. Chakrabartty, J. A. Schellman and R. L. Baldwin, Large differences in the helix propensities of alanine and glycine, *Nature*, 1991, **351**, 586–588.

24 L. Whitmore and B. A. Wallace, Protein secondary structure analyses from circular dichroism spectroscopy: Methods and reference databases, *Biopolymers*, 2008, **89**, 392–400.

25 W. Lee, M. Tonelli and J. L. Markley, NMRFAM-SPARKY: Enhanced software for biomolecular NMR spectroscopy, *Bioinformatics*, 2015, **31**, 1325–1327.

26 M. D. Hanwell, D. E. Curtis, L. D. C, T. Vandermeersch, E. Zurek and G. R. Hutchinson, Avogadro: an advanced semantic chemical editor, visualization, and analysis platform, *J. Cheminform.*, 2012, **4**, 17.

27 M. J. Abraham, T. Murtola, R. Schulz, S. Páll, J. C. Smith, B. Hess and E. Lindah, Gromacs: High performance molecular simulations through multi-level parallelism from laptops to supercomputers, *SoftwareX*, 2015, **1**–**2**, 19–25.

28 A. D. Mackerell Jr., N. Banavali and N. Foloppe, Development and Current Status of the CHARMM Force Field for Nucleic Acids, *Biopolym. Orig. Res. Biomol.*, 2001, **56**, 257–265.

29 K. Vanommeslaeghe, E. Hatcher, C. Acharya, S. Kundu, S. Zhong, J. Shim, E. Darian, O. Guvench, P. Lopes, I. Vorobyov and A. D. Mackerell Jr., CHARMM general force field: A force field for drug-like molecules compatible with the CHARMM all-atom additive biological force fields, *J. Comput. Chem.*, 2010, **31**, 671–690.

30 S. Marqusee, V. H. Robbins and R. L. Baldwin, Unusually stable helix formation in short alanine-based peptides., *Proc. Natl. Acad. Sci. U. S. A.*, 1989, **86**, 5286–5290.

31 A. Chakrabartty, T. Kortemme and R. L. Baldwin, Helix propensities of the amino acids measured in alanine-based peptides without helix-stabilizing side-chain interactions, *Protein Sci.*, 1994, **3**, 843–852.

32   S. Hwang, Q. Shao, H. Williams, C. Hilty and Y. Q. Gao, Methanol Strengthens Hydrogen Bonds and Weakens Hydrophobic Interactions in Proteins - A Combined Molecular ... Methanol Strengthens Hydrogen Bonds and Weakens Hydrophobic Interactions in Proteins À A Combined Molecular Dynamics and NMR study, *J. Phys. Chem. B*, 2011, **115**, 6653–6660.

33   K. Wüthrich, *NMR of Proteins and Nucleic Acids*, John Wiley & Sons, Inc., New York, 1986.

34   D. S. Wishart, B. D. Sykes and F. M. Richards, The Chemical Shift Index: A Fast and Simple Method for the Assignment of Protein Secondary Structure Through NMR Spectroscopy, *Biochemistry*, 1992, **31**, 1647–1651.

35   C. A. López, A. H. de Vries and S. J. Marrink, Amylose folding under the influence of lipids, *Carbohydr. Res.*, 2012, **364**, 1–7.

36   G. Ozer, S. Quirk and R. Hernandez, Thermodynamics of Decaalanine Stretching in Water Obtained by Adaptive Steered Molecular Dynamics Simulations, *J. Chem. Theory Comput.*, 2012, **8**, 4837–4844.

37   E. M. Meiering, The threat of instability: Neurodegeneration predicted by protein destabilization and aggregation propensity, *PLoS Biol.*, 2008, **6**, 1383–1385.

38   S. Walter, B. Hubner, U. Hahn and F. X. Schmid, Destabilization of a protein helix by electrostatic interactions, *J. Mol. Biol.*, 1995, **252**, 133–143.

39   G. Desiraju and T. Steiner, *The weak hydrogen bond in structural chemistry and biology*, Oxford University Press/International Union of Crystallography, Oxford, 2001.

40   N. Trinajstić, Calculation of carbon-sulphur bond lengths, *Tetrahedron Lett.*, 1968, **9**, 1529–1532.

41   J. López-Llano, L. A. Campos, J. Sancho and J. Sancho, α-helix stabilization by alanine relative to glycine: Roles of polar and apolar solvent exposures and of backbone entropy, *Proteins Struct. Funct. Genet.*, 2006, **64**, 769–778.

42   A. Grauer and B. König, Peptidomimetics - A versatile route to biologically active compounds, *European J. Org. Chem.*, 2009, 5099–5111.

43   W. S. Horne, M. K. Yadav, C. D. Stout and M. R. Ghadiri, Heterocyclic peptide backbone modifications in an α-helical coiled coil, *J. Am. Chem. Soc.*, 2004, **126**, 15366–15367.

44   L. R. Whitby, Y. Ando, V. Setola, P. K. Vogt, B. L. Roth and D. L. Boger, Design, Synthesis, and Validation of a β-Turn Mimetic Library Targeting Protein-Protein and Peptide-Receptor Interactions, *J. Am. Chem. Soc.*, 2011, **133**, 10184–10194.

45   S. Deike, S. Rothemund, B. Voigt, S. Samantray, B. Strodel and W. H. Binder, β-Turn mimetic synthetic peptides as amyloid-β aggregation inhibitors, *Bioorg. Chem.*, 2020, **101**, 104012.

TABLES

Table 1. Amino acid sequences of peptides used in this work, where A_{ox} indicates the presence of an oxetane-modified alanine residue and G_{ox} indicates the presence of an oxetane-modified glycine residue. Measurements were made in three different solvents: 10 mM potassium phosphate, pH 7.0 + 1M NaCl (5°C); 80% MeOH (5°C); 100% MeOH (0°C). Percentage helical content was obtained from fitting of the data using DichroWeb[24], and these values were used to estimate the number of helical residues in the 18-residue peptide. Numbers in brackets represent the number of residues that are "unfolded" by the incorporation of an oxetane at a single position.

Peptide	Sequence								
1	Ac-KAAAAKAAAAKAAAAKGY-NH$_2$								
2a	Ac-KAAAAKAA$_{ox}$AAKAAAAKGY-NH$_2$								
2b	Ac-KAA$_{ox}$AAKAAAAKAAAAKGY-NH$_2$								
2c	Ac-KAG$_{ox}$AAKAAAAKAAAAKGY-NH$_2$								
	KP$_i$ (pH 7.0, (5°C)			**80% MeOH (5°C)**			**100% MeOH (0°C)**		
Peptide	$[\theta]_{222}$	% Helix	Helical res.	$[\theta]_{222}$	% Helix	Helical res.	$[\theta]_{222}$	% Helix	Helical res.
1	-20655	58	10	-19239	56	10	-19861	57	10
2a	487	4	1 (-9)	-2483	12	2 (-8)	-4394	15	3 (-7)
2b	-1443	9	2 (-8)	-10813	34	6 (-4)	-10496	34	6 (-4)
2c	-1170	9	2 (-8)	-8262	27	5 (-5)	-10902	37	7 (-3)

Table 2. Partial ^{1}H chemical shift assignments for peptides **1** and **2c** solubilised in 80% MeOD-d_4 + 20% H_2O to a final peptide concentration of 2 mM. Due to the repetitive nature of the sequence, sequential assignment was not possible for the majority of residues. Unique residues were readily identified and sequentially assigned, and NOE data was used where possible to sequentially assign additional residues. Lys residues followed by multiple sequence positions have been assigned by residue type, but not by position, so all possible sequence positions are noted.

Peptide 1	Hα	Hβ	Hδ	Hε	Hγ	NH
Lys (Lys 1, 6, 11)	4.05	1.86	1.73	2.97	1.50	8.70
Lys' (Lys 1, 6, 11)	4.02	2.00	1.70	2.92		8.24
Lys" (Lys 1, 6, 11)	4.03	1.99	1.70	2.92		8.19
Ala15	4.18	1.55				8.10
Lys16	4.26	1.96	1.68	2.95	1.53	7.66
Gly17	4.00					7.99
Tyr18	4.52	2.85/3.11				7.96
Peptide 2c	Hα	Hβ	Hδ	Hε	Hγ	NH
Lys1	4.26	1.84	1.71	2.97	1.49	8.40
Ala2	4.30	1.42				8.46
Gly-ox3	3.65	4.12				8.22
Ala4	4.25	1.49				8.72
Lys (Lys 6, 11)	4.14	1.88	1.73	2.96	1.57	8.78
Lys" (Lys 6, 11)	4.22	1.97	1.70	2.94		8.14
Ala15	4.19	1.55				8.09
Lys16	4.26	1.95	1.69	2.94	1.50	7.68
Gly17	4.00					8.01
Tyr18	4.53	2.85/3.12				7.97

FIGURE LEGENDS

Figure 1. Circular dichroism spectra acquired for 0.1 mg/mL solutions of each peptide shown in Table 1 in **(A)** 10 mM potassium phosphate buffer (pH 7.0) with 1M NaCl at 5°C, **(B)** 80% methanol / 20% water at 5°C, and **(C)** 100% methanol at 0°C. Negative peaks at 208 and 222 nm indicate the presence of α-helical protein structure.

Figure 2. Work required to pull parent and oxetane-modified helices by 5 nm (20 ns) of simulation. The parent peptide (**1**) requires the most work to unwind and the centrally modified peptide (**2a**) requires the least work to unwind. The N-terminally modified peptides (**2b** and **2c**) require similar amounts of work to unwind, although the A_{ox} modification (**2b**) requires slightly less than the G_{ox} peptide (**2c**) ($p < 0.02$ when compared using independent samples t-test). Error bars represent standard error between 10 repeats, difference between all four data sets $p < 0.0001$ when compared using One-Way ANOVA.

Figure 3. Snapshots of representative helical peptides taken at 5 ns, close to the start of the simulation. Helical structures for **1** (purple), **2a** (green), **2b** (cyan) and **2c** (pink) show clear kinking in proximity to the oxetane modification, as well as changes in the hydrogen bonding (represented with dashed lines) patterns about and downstream of the modification.

Figure 4. Ramachandran plots for residues affected by the introduction of oxetane for **(A)** modification of peptides **2b** and **2c** at residue 3, and **(B)** modification of peptide **2a** at residue 8. ϕ and ψ angles were plotted for each residue from 2 to 5 ns. Each plot contains data from 10 repeats. The position of the oxetane modification is indicated with an asterisk.

Figure 5. Representative plots indicating number of hydrogen bonds per residue over 20 ns. Modified sites are indicated with an arrow. There is distortion up to four residues away from the site of modification.

Figure 6.

Snapshots of **(A) 1** (purple), **(B) 2a** (green), **(C) 2b** (cyan) and **(D) 2c** (pink) helical peptides taken at 5 ns intervals, highlighting the key unwinding events. In all cases, helicity is completely lost after 25 ns of simulation. Each peptide was anchored at by the Cα atom of Lys1, and pulled by the Cα atom of Tyr18, as indicated by arrows on the left-hand side.
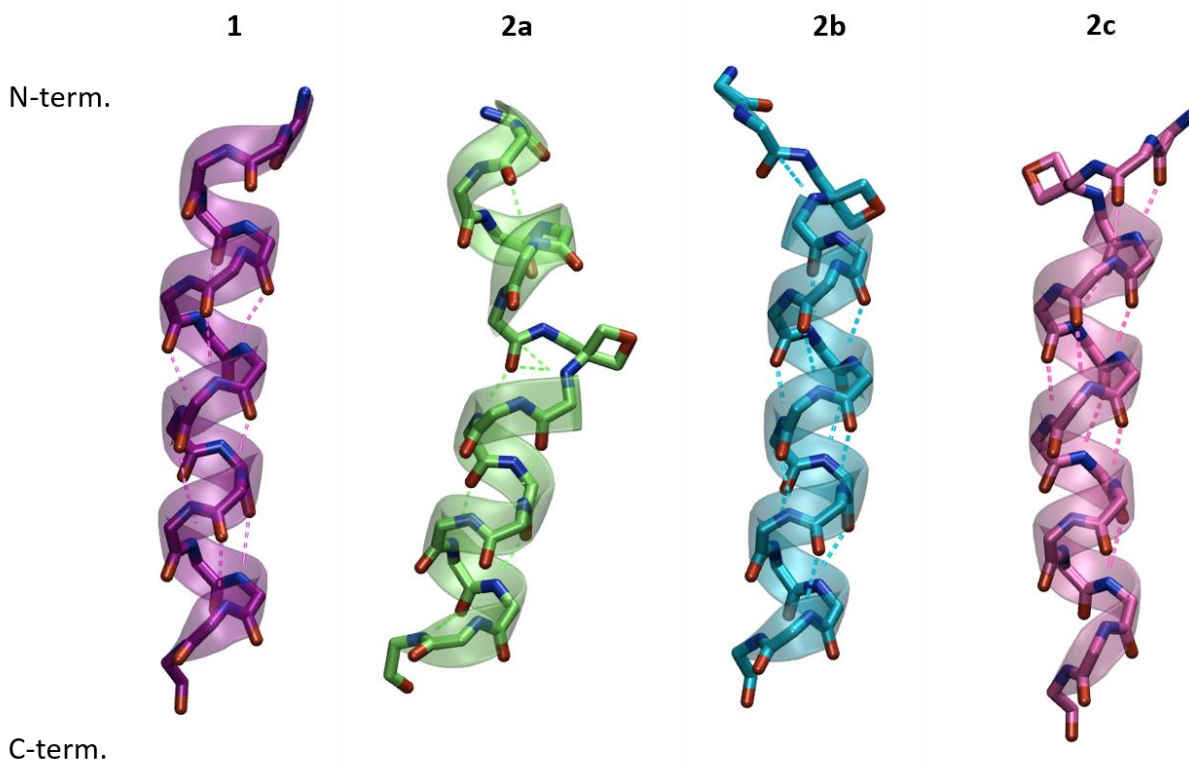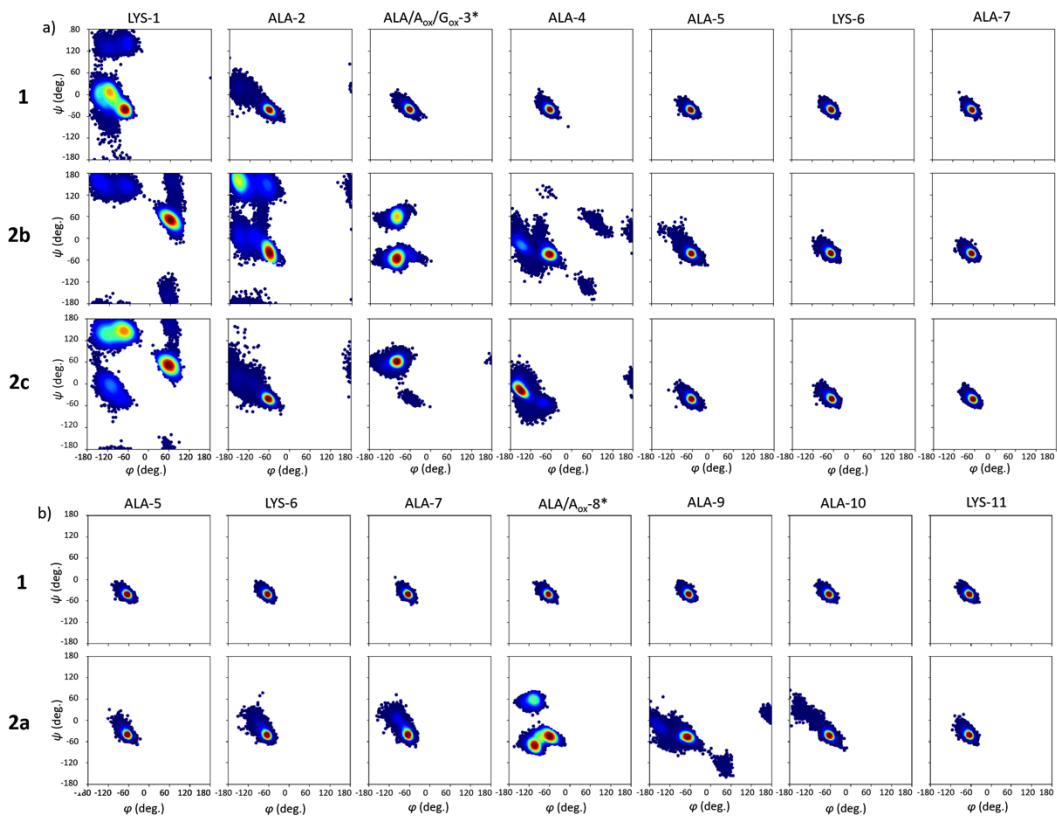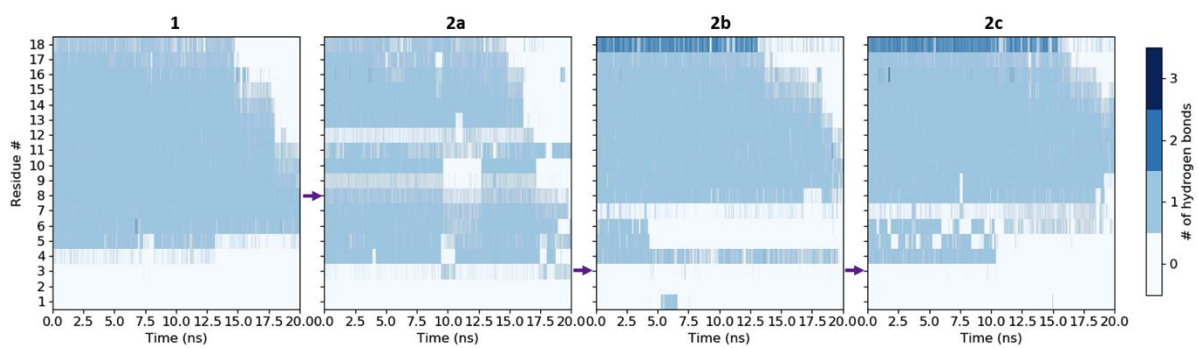
FIGURES

Figure 1.
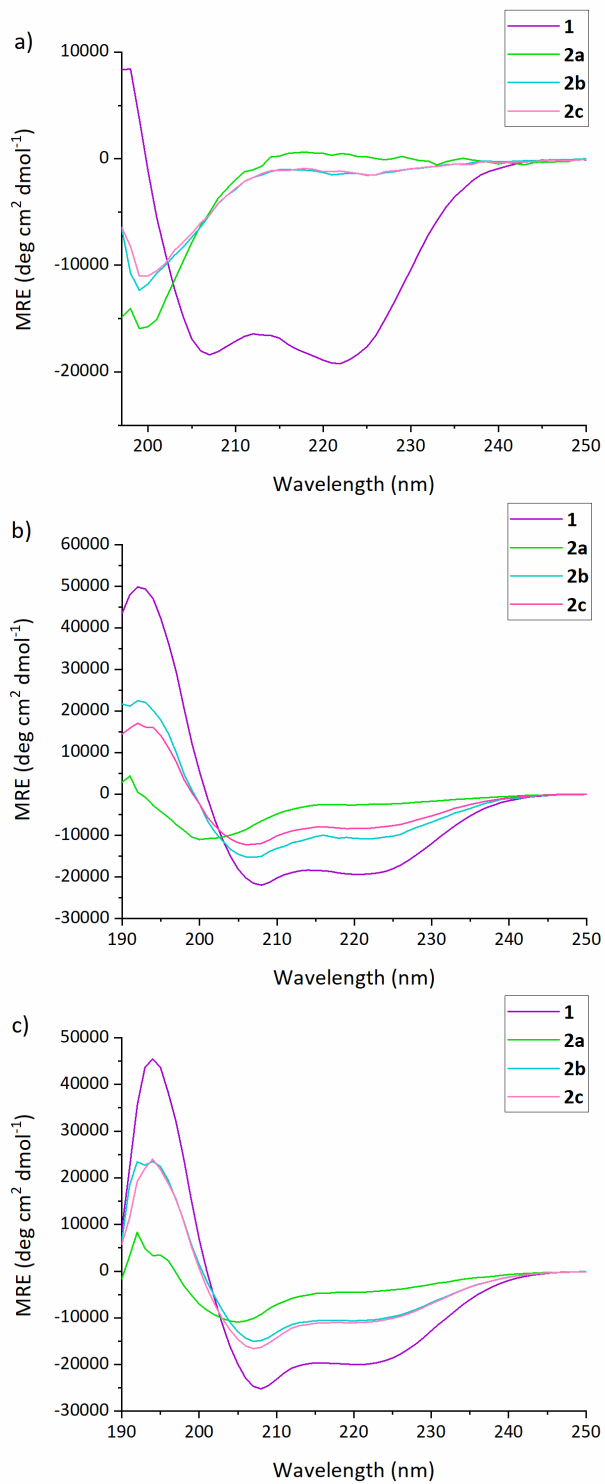
Figure 2.
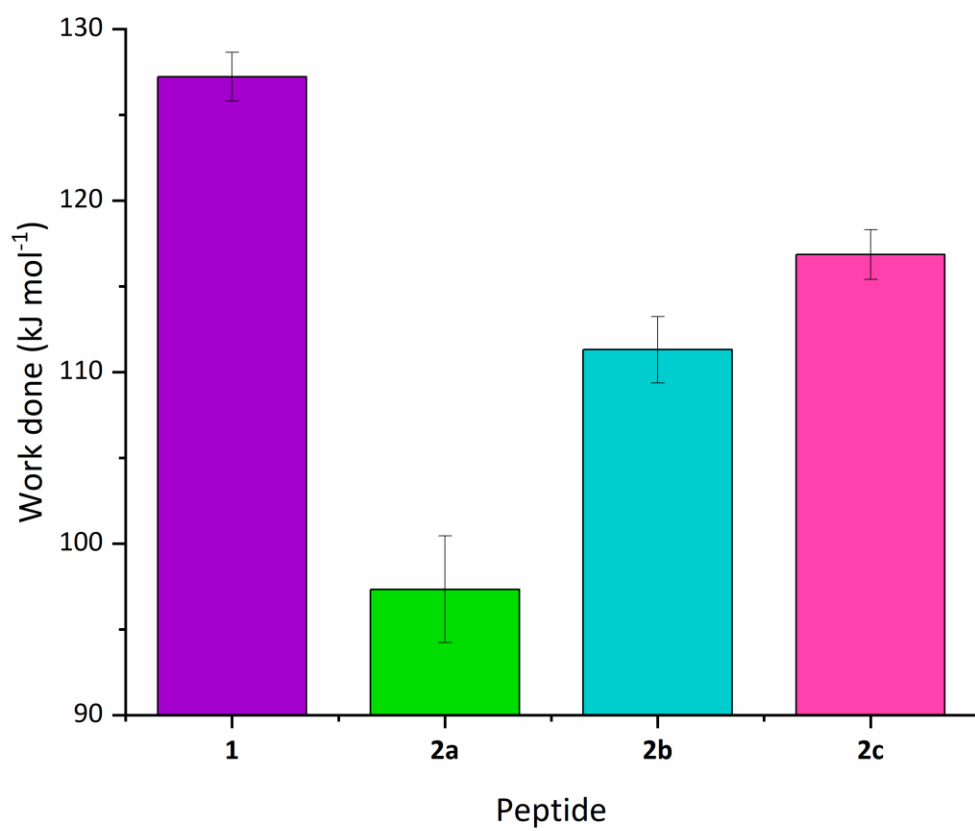
Figure 3.

Figure 4.

Figure 5.

Figure 6.